# Skinergy: Machine-Embroidered Silicone-Textile Composites as On-Skin Self-Powered Input Sensors


Tianhong Catherine Yu
ty274@cornell.edu
Hybrid Body Lab, Cornell University
Ithaca, New York, USA

Nancy Wang*
sw664@cornell.edu
Hybrid Body Lab, Cornell University
Ithaca, New York, USA

Sarah Ellenbogen*
sje57@cornell.edu
Hybrid Body Lab, Cornell University
Ithaca, New York, USA

Hsin-Liu (Cindy) Kao
cindykao@cornell.edu
Hybrid Body Lab, Cornell University
Ithaca, New York, USA


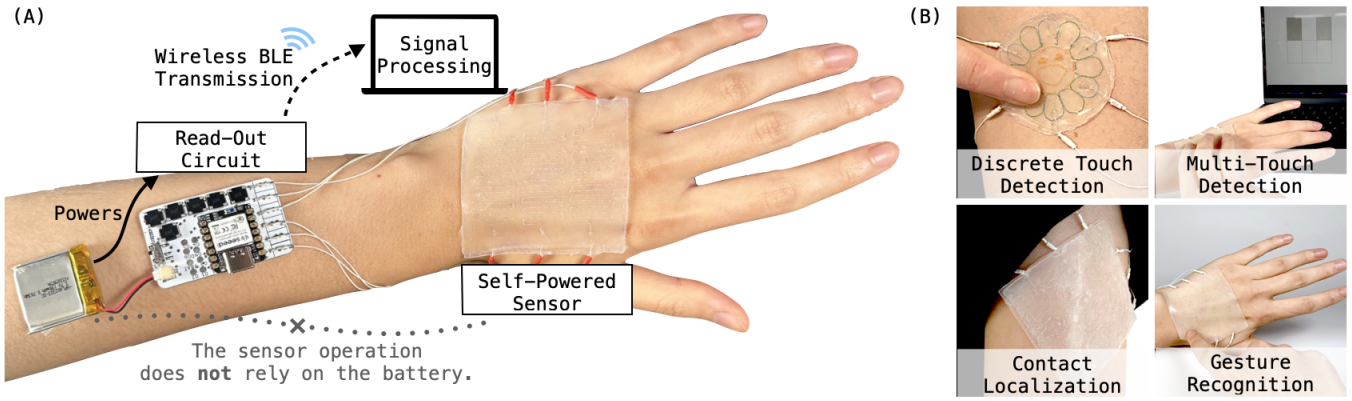


**Figure 1: (A) Skinergy centers around the triboelectric nanogenerator (TENG) on-skin sensors which do not rely on external power for sensor operation. The sensing board, which still requires a battery, reads the signals generated by the sensor and transmits the signals wirelessly to a nearby computer for signal processing. (B) Depending on the TENG electrode design, Skinergy is capable of discrete touch detection, multi-touch detection, contact localization, and gesture recognition.**


## ABSTRACT

We propose Skinergy for self-powered on-skin input sensing, a step towards prolonged on-skin device usages. In contrast to prior on-skin gesture interaction sensors, Skinergy's sensor operation does not require external power. Enabled by the triboelectric nanogenerator (TENG) phenomenon, the machine-embroidered silicone-textile composite sensor converts mechanical energy from the input interaction into electrical energy. Our proof-of-concept untethered sensing system measures the voltages of generated electrical signals which are then processed for a diverse set of sensing tasks: discrete touch detection, multi-contact detection, contact localization, and gesture recognition. Skinergy is fabricated with off-the-shelf materials. The aesthetic and functional designs can be easily customized and digitally fabricated. We characterize Skinergy and conduct a 10-participant user study to (1) evaluate its gesture recognition performance and (2) probe user perceptions and potential applications. Skinergy achieves 92.8% accuracy for a 11-class gesture recognition task. Our findings reveal that human factors (*e.g.*, individual differences in skin properties, and aesthetic preferences) are key considerations in designing self-powered on-skin sensors for human inputs.



## CCS CONCEPTS

• **Human-centered computing** → **Human computer interaction (HCI)**; **Ubiquitous and mobile computing**.

**ACM Reference Format:**
Tianhong Catherine Yu, Nancy Wang, Sarah Ellenbogen, and Hsin-Liu (Cindy) Kao. 2023. Skinergy: Machine-Embroidered Silicone-Textile Composites as On-Skin Self-Powered Input Sensors. In *The 36th Annual ACM Symposium on User Interface Software and Technology (UIST '23), October 29–November 01, 2023, San Francisco, CA, USA.* ACM, New York, NY, USA, 15 pages. https://doi.org/10.1145/3586183.3606729


*Both authors contributed equally to this research.



*UIST '23, October 29–November 01, 2023, San Francisco, CA, USA*



ACM ISBN 979-8-4007-0132-0/23/10…$15.00
https://doi.org/10.1145/3586183.3606729


## 1 INTRODUCTION

On-skin interfaces afford always-available interactions towards intrinsic human augmentation. These skin-conformable devices present promising applications ranging from haptic feedback [15, 26], physiological and biomedical sensing [40, 57], visual displays [21, 60, 63] to drug delivery [47]. While recent research in Human-Computer Interaction (HCI) [21, 22, 62, 63] and the field of material science [25] have developed skin-conformable circuitry

and substrates, prolonged battery life remains a shared challenge among on-skin electronics due to their miniaturized and soft nature. A short battery life demands frequent recharging that is inconvenient.

In this work, we explore self-powered on-skin input sensors with Skinergy (Figure 1): a biomechanical energy harvester that powers its own sensing operation. Touch-based input interactions [20, 27, 41, 49, 55, 69] are an integral channel for controlling on-skin and other ubiquitous computing devices. Our self-powered on-skin input sensors function similarly to human skin receptors: given external stimuli, skin receptors fire action potentials which are electrical signals that are then processed by human brains. In parallel, given touch-based interactions, Skinergy **generates voltage potential** which are electrical signals that are then processed by micro-controllers. Note, Skinergy only features a self-powered sensor and still requires an externally powered system (e.g., the micro-controller) to process the signals.

Skinergy is enabled by the triboelectric nanogenerator (TENG) phenomenon[10]. TENGs are fast gaining traction as they efficiently convert mechanical energy into electrical power from ample everyday human motions and activities. As a result of triboelectrification and triboelectrostatic induction, mechanical energy from touch-based interactions can be converted into electrical energy. On-skin input sensing from prior works requires supplying DC or AC voltages depending on the chosen resistive [62] or capacitive sensing [41] modalities. Without supplying additional voltages, Skinergy generates electrical energy, which can then be processed for a diverse set of sensing tasks: discrete touch detection, multi-contact detection, contact localization, and gesture recognition.

Using accessible off-the-shelf materials, digital embroidery machines, and consumer 3D printers, Skinergy silicone-textile composites TENGs are fabricated at low cost with the potential to scale. To the best of our knowledge, Skinergy presents the *first* on-skin TENG sensor and the *first* untethered wearable TENG sensing system for human inputs within the Human-Computer Interaction (HCI) community.

To maximize energy harvesting capabilities, the fabrication of TENGs typically involves highly functional materials that are expensive and require proprietary equipment to process and synthesize [72]. Also, sensor measurements are made with large and/or expensive apparatus (*e.g.*, oscilloscopes and current preamplifiers). In our work, we employ an HCI human-centered lens towards self-powered sensing applications: an **untethered on-skin sensing system** that is **appropriate for the on-skin context**, **user friendly in fabrication without needed propriety and expensive equipment and materials**, and **easily customizable** both in terms of functionality and aesthetics.

To achieve such sensing systems, we fabricate soft and stretchable silicone-textile composites that are comfortable for on-skin wear. We first embroider on Polyvinyl chloride (PVC) sheets and tear-away stabilizers using conductive threads for electrode patterns and conventional rayon threads for aesthetic designs. The PVC sheets and stabilizers are later removed. We then cast silicone rubber onto the embroidered substrate using 3D-printed molds. The composites are around 700 microns thick. Our supporting converter software streamlines the digital fabrication process with digital embroidery and 3D printing. As a proof of concept, we prototype a wearable untethered wireless readout circuit that measures the voltage potentials for each sensing electrode. The measured voltages are sent to a nearby computing device (*e.g.*, a computer) for processing via Bluetooth.

For evaluation, we characterize Skinergy's load resistance-voltage profile, electrode shape effects, pressure & spatial sensitivity, and stretchability & repeatability. We also conduct a 10-participant user study. In the quantitative studies, our machine-learning algorithm achieved 92.8% accuracy for 11-class gesture recognition. In the qualitative studies, we probe user perceptions and potential applications of self-powered on-skin sensors. Both of the studies revealed that **human factors** like individual differences in skin properties and aesthetic preferences are key considerations in designing such sensors. We summarized our contributions below:

- We describe the sensing principles of Skinergy, our silicone-textile composites triboelectric nanogenerators (TENGs).
- We present a digital fabrication process for easily customizable on-skin self-powered input sensors and characterize Skinergy.
- We conduct a 10-participant quantitative and qualitative user study to evaluate Skinergy's proof-of-concept untethered sensing system.
- We demonstrate example real-time applications of Skinergy.

## 2 BACKGROUND AND RELATED WORK

We divide the background and related work into three subsections: (1) on-skin input sensing, the functionality of Skinergy; (2) triboelectric nanogenerators, the phenomenon that enables Skinergy' self-powered sensing; and (3) machine embroidery for interactive device fabrication, the digital fabrication method of Skinergy.

### 2.1 On-Skin Input Sensing

On-skin sensing is attractive to applications spanning from biomedical monitoring [57] and motion tracking [59] to Human-Computer Interaction (HCI). The HCI community started studying on-skin input sensing in 2015 with iSkin, a stretchable skin overlay that supports single and multi-touch fabricated with layers of PDMS and carbon-filling PDMS (cPDMS) [62]. Researchers embed miniaturized electronics or conductive materials into skin-friendly substrates [17, 22, 35, 66] to create on-skin sensors. Popular sensing modalities include piezoresisitve [55, 62] and capacitive sensing [21, 34, 41, 63, 69]. In PDMSkin, resistive sensing along with machine learning enabled gesture recognition [49]. The piezoresistive and capacitive sensing can be combined for richer interactions [32, 63]: squeeze sensors, strain gauge, etc. However, all of these sensors require the injection of electrical power. Skinergy is the first in HCI to explore self-powered on-skin sensors, meaning the sensed events power the sensor itself. It is able to achieve similar gestural interaction capabilities to those of prior works, showcasing promising a solution to prolonged battery life.

### 2.2 Triboelectric Nanogenerators for Self-Powered Sensing

The triboelectric Nanogenerators(TENGs) phenomenon is the result of the combination of triboelectrification and triboelectrostatic induction. There are four TENGs modes: contact-separation mode,

lateral sliding mode, single electrode mode, and freestanding triboelectric layer mode. Skinergy uses the single electrode mode in which the charge transfers between the positively charged human skin and the negatively charged silicone rubber are picked up by conductive threads and thus creating AC signals. TENGs have been used in several self-powered HCI contexts: paper interfaces [6, 23], 3D tangible interaction [31], interactive plywood [67], textile sensors for human motions [24], deformable chord sensor [53], and microphone [3]. Our work has a different context: on-skin interaction. The slim and flexible form factors have additional design considerations and constraints while ensuring the sensing performance. The SI-TENG is the most similar work to ours: three-ply twisted silver-coated conductive nylon yarn is routed in serpentine patterns, fixed by nails and laser-cut acrylic plates, and embedded into silicone rubber to enable on-skin touch events detection and touch localization [8]. In this paper, we extend self-powered on-skin sensing with touch gesture classification using machine learning techniques. Furthermore, we digitize the fabrication process focusing on wearability and evaluate the sensor with a proof-of-concept implementation.

## 2.3 Machine-Embroidery for Interactive Device Fabrication

Embroidery is a process that uses needles and threads to create patterns on substrates, typically textiles. Along with conductive [4] and functional (e.g., shape memory alloy [38]) fibers, embroidery is a popular fabrication technique to create smart textiles. Computerized embroidery machines further allow users to precisely control the patterns numerically. These machines are inexpensive and easy to control, yet they offer a large design space [28], making them suitable for prototyping e-textiles [14, 19] and on-skin interfaces [18] with high fidelity [12]. For our on-skin sensing purpose, machine-embroidered traces are more electrically & mechanically durable than screen-printed traces [32], more time-efficient and less manual than hand-weaving with jigs [8], and more reproducible than routing threads by hands. In 2000, machine-embroidering conductive threads as capacitive sensing electrodes was an early embodiment of clothing as wearable computers[45]. Since then, researchers have explored embroidered resistive [2] and capacitive [1] sensors, speakers [46], near-field communication [71] and powering [29] antennas, liquid crystal textile displays [9], tangible input buttons [11], etc. Recently, machine embroidery was used to fabricate textile-based TENGs at scale. Sala de Medeiros et al. used machine-embroidered patterns with cotton threads to cover the triboelectric layers and silver norfloxacin (AgNF) electrodes [51]. The embroidered pattern is further rendered omniphobic with spray silanization so that the TENG becomes waterproof and antibacterial. Though using the same machinery, we machine-embroider the triboelectric layers and electrodes with off-the-shelf conductive thread, water-soluble thread, and conventional thread. Chen et al. used cotton threads and triboelectric threads, plied enameled wires with plasma treatment, to embroider single-electrode TENGs. When the TENG threads, with positive negative electron affinity, are in contact with Polytetrafluoroethylene (PTFE) which has negative electron affinity, they are used for self-powered sensing and energy harvesting. In contrast, Skinergy is designed to be worn

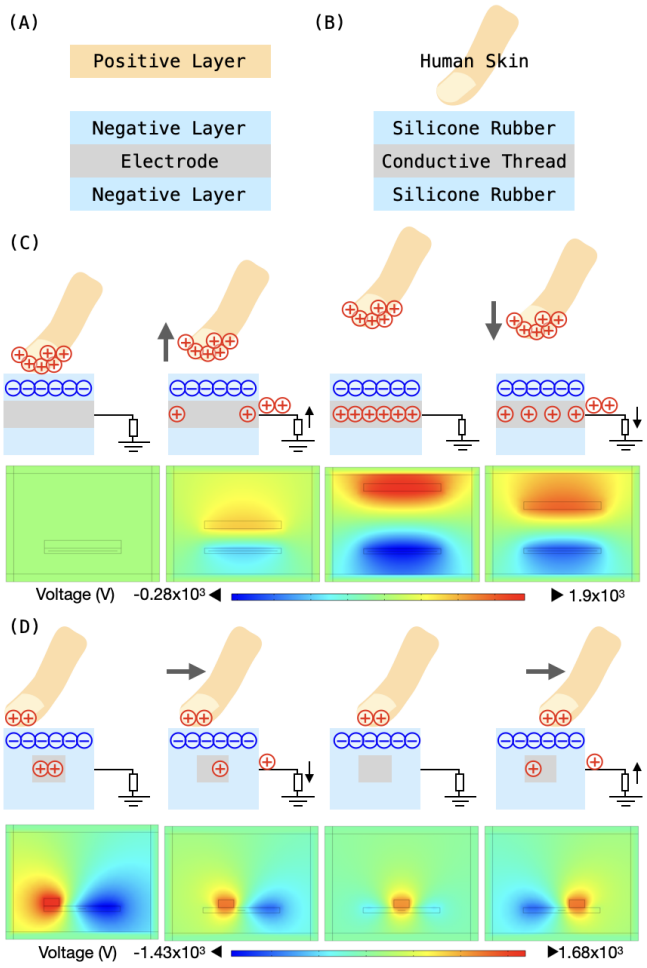


**Figure 2: Sensing principle of Skinergy. (A): the single-mode TENGs topology; (B): our TENGs material selection; (C): the schematic of the contact-separation mechanism; (D): the schematic of the sliding mechanism. The two schematics demonstrate the AC current formations and the respective potential distribution simulation using COMSOL. Note that the simulation uses parameters close to our selected materials, and the voltage distribution depends on the device size. Therefore, the absolute voltage distributions are inaccurate, but the relative voltage distribution is accurate.**

on-skin and used in interaction with skin which has positive electron affinity. Moreover, we propose a novel fabrication process for machine-embroidering multi-layered silicone-textile composites using water-soluble thread and PVC sheets as the sacrificial layer.

# 3 THEORY OF OPERATION

Wu et al. defines a self-powered sensor (like Skinergy) as a sensor that (1) automatically gives out an electric signal when mechanically triggered (gesture events) without an external power source and that (2) the operation power source provided for the sensor is self-generated [68]. Skinergy uses the triboelectric nanogenerator

(TENG) single electrode mode containing an electrode material, a relatively negatively charged dielectric material, and a relatively positively charged dielectric material, shown in Figure 2A. In Skinergy's design, conductive thread, silicone rubber, and human skin function as the electrode, the negative layers, and the positive layer, respectively (Figure 2 B). The conductive thread electrode is connected to the reference ground (GND) via a load resistor (Figure 2C-D). AC signals flow through the load resistor when contact-separation and sliding motions occur.

*Contact-Separation Mechanism.* Illustrated in Figure 2C, when the finger is in contact with the device, there is negligible electrical potential between the skin and silicone rubber. The triboelectric effect occurs as the finger moves away from the device, and positive charges are transferred from the skin to the conductive thread electrode. The charge transfer prompts electrons to flow, generating an instantaneous electrical current until the positive charges on the conductive yarn are equal to those on the silicone rubber. At this point, the finger and the device are fully separated, the sensor is at equilibrium, and thus there are no electrical signals. When the finger moves toward the device, the positively charged conductive yarn returns the positive charges back to the finger due to electrical potential differences. Note that in this stage, the instantaneous electrical current generated is in a different direction from when the finger is moving away from the device. Finally, when the finger touches the sensor again, the cycle finishes. To summarize, **the contact-separation cycle generates AC signals as the finger touches and leaves the sensor**.

*Sliding Mechanism.* Figure 2D illustrates a different mechanism of the finger **sliding across the conductive thread generates AC signals as the finger moves towards and away from the electrode**. Similarly to the contact-separation mechanism, as the finger approaches the electrode, the conductive thread becomes less positively charged. The conductive thread becomes more positively charged as the finger moves away from the electrode.

COMSOL simulations of open circuit potential distribution further show that human inputs can be detected from measuring and processing voltage differences across the load resistor.

## 4 FABRICATING SKINERGY

The rapid prototyping process of Skinergy silicone-textile composites includes first designing the shape, look, and functionality of the self-powered sensor (Sec 4.1), then machine-embroidering the conductive and decorative threads onto the prepared substrate (Sec 4.2) and finally casting silicone over the embroidered substrates into desired shapes using the 3D-printed mold (Sec 4.3). Silicone functions both as the negative dielectric TENG material and as insulation between the skin and the electrode.

### 4.1 Supporting Converter Software

Most embroidery software is proprietary and costly at thousands of dollars. In recent years, there are open-sourced digital embroidery libraries (*e.g.*, computational embroidery with Processing [1]) and graphical user interfaces (*e.g.*, Inkscape plug-in Ink/Stitch [2]). While these open-source tools are fairly easy to use, they are still more complicated to access than simple graphic design software. Furthermore, for the fabrication of Skinergy sensors, the embroidery design is accompanied by a 3D model of a mold with a predefined shape and thickness.

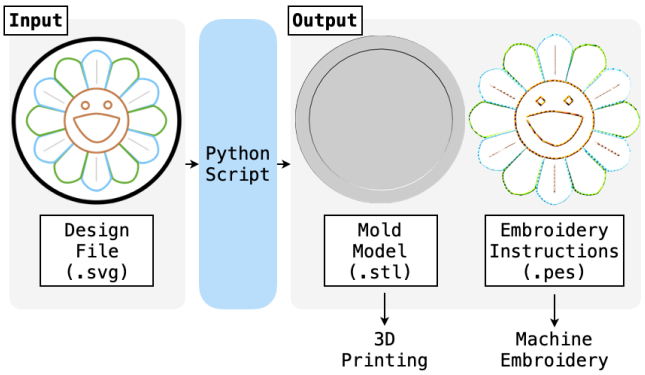


**Figure 3: Supporting converter software for digital fabrication. To streamline the design process, users can design the shape (thick black lines), electrode placements (thin gray lines), and aesthetics (other lines, green, blue, and brown in this case) of Skinergy sensors in a single vector graphic file (.svg). Our python script then outputs the mold model (.stl) and the embroidery instructions (.pes) that can be directly used for 3D printing and machine embroidery, respectively. The embroidery instructions are visualized using Ink/Stitch.**

To streamline the process of manually creating the mold model and the embroidery instructions, we implemented a supporting software converter in Python (Figure 3). The converter takes a SVG file that can be designed in vector graphic design software like Adobe Illustrator, and outputs:

- A mold model (.stl) for 3D printing: The thick black strokes in the input design file define the shape and size of the mold. Users can specify the thickness of the mold in the converter.
- Embroidery instructions (.pes) for machine embroidery: The thin gray strokes define the electrode designs. Strokes with other colors define aesthetic designs.

The converter uses `svgpathtools`[3] for SVG parsing, `SolidPython`[4] for model creation, and `pyembroidery`[5] for embroidery instructions generation. The script is included in the supplemental material.

### 4.2 Machine Embroidery

We load the embroidery instructions output from the converter into the digital embroidery machine. First, we prepare the setup for machine embroidery.

***Embroidery Machine Setting.*** We attach the SCHMETZ microtex needle (professional grade, 103/705 H-M CF, 70/10) to the machine (Brother SE600 Home Sewing and Embroidery Machine). The thread tension is set at 4.

***Embroidery Substrate.*** We secure one layer of tear-away stabilizer (Sulky Iron-On Tear-Away Stabilizer) on the embroidery hoop and

[1] https://github.com/CreativeInquiry/PEmbroider
[2] https://inkstitch.org/
[3] https://github.com/mathandy/svgpathtools
[4] https://github.com/jeff-dh/SolidPython
[5] https://github.com/EmbroidePy/pyembroidery

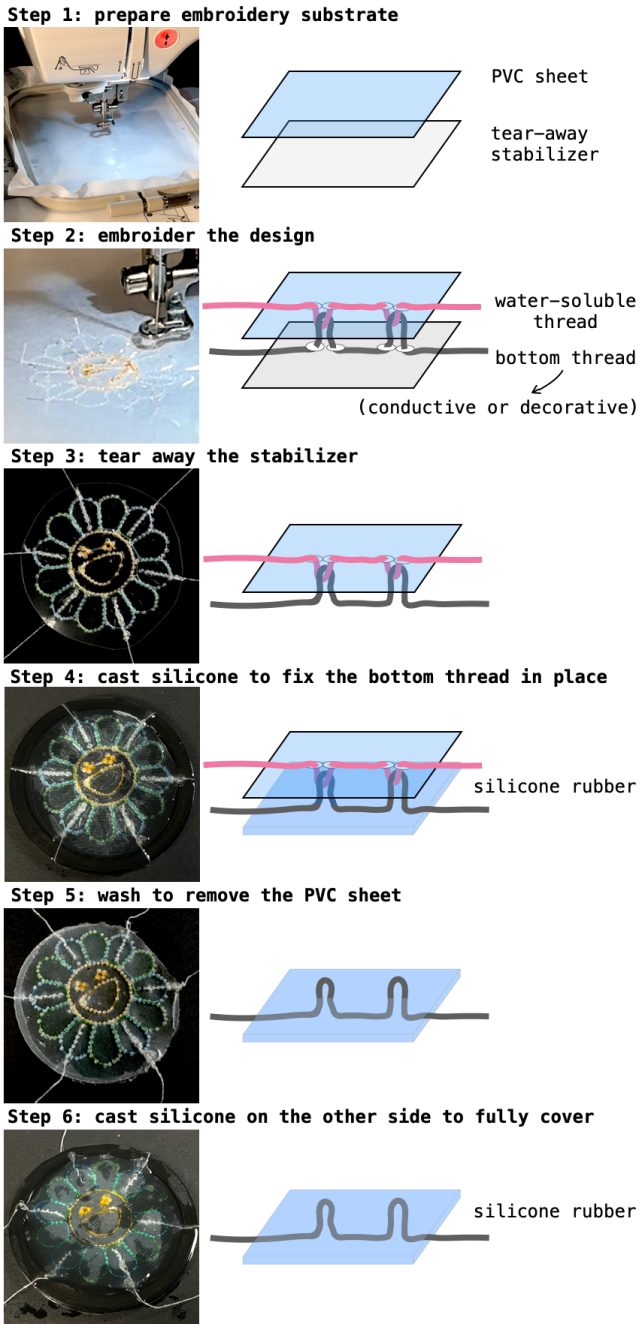


**Figure 4: Step-by-step fabrication workflow. (1) Prepare the embroidery substrate with PVC sheet and the tear-away stabilizer; (2) Embroider the design; (3) Tear away the stabilizer; (4) Cast silicone to fix the top thread in place; (5) Wash away the water-soluble stabilizer to remove the PVC sheet; (6) Cast silicone on the other side to fill the holes.**

tape a sheet of clear PVC plastic (plastic file folders) on the stabilizer (Step 1 in Figure 4).

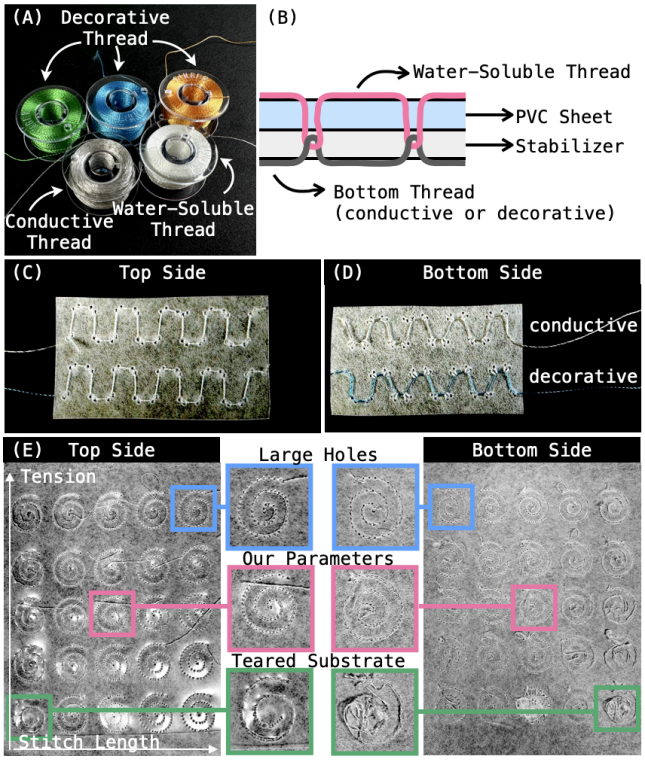


**Figure 5: Components of the embroidered substrate. (A) Threads in use. (B) Illustration of the bottom thread held by the top water-soluble thread. (C) The top side of the embroidered substrate with the water-soluble thread and PVC sheet on the top. (D) The bottom side of the embroidered substrate with the bottom thread, conductive or decorative, and stabilizer on the bottom. (E) Embroidery tension and stitch length setting matrix. High tension and stitch length result in large holes. Low tension and stitch length result in a torn substrate.**

***Embroidery Threads.*** As shown in Figure 5A-D, we use a PVA filament water-soluble thread (Superior Threads - Vanish-Extra Water Soluble Thread) as the upper embroidery thread and a conductive silver-plated nylon thread (LessEMF, <100 Ohm/1cm) or conventional thread as the lower embroidery thread. After the setup, embroidery begins (Step 2 in Figure 4). Aesthetic designs with conventional rayon threads are first embroidered. To leave ends for electrical connections for the conductive threads, at the end of each conductive path, we pull out the tail and manually cut it instead of using the built-in trim, where the tail will be too short for connection. After all paths are embroidered, we remove the substrate from the hoop and tear away the stabilizer (Step 3 in Figure 4).

*4.2.1 Embroidery Parameters.* Embroidery machines are typically designed to have a neat top pattern and do not pay much attention to thread paths below. However, our conductive traces are embroidered on the bottom side of the substrate. To optimize for clean

bottom paths, we found turning the stitch length and the tension have the greatest effects.

We show a matrix (Figure 5E) with tensions ranging from 0 to 8 with increments of 2 and stitch lengths ranging from 2mm to 4mm with increments of 0.4mm. The matrix exhibits mostly unfit stitch length-tension pairs and a few suitable choices and serves as a reference for optimizing both factors while embroidering. A low stitch length corresponds to high thread tension, higher stitch density, and larger punctured holes. The optimal stitch length-tension pair results in minimal puncture size and clean threads on both sides of the substrate, creating the most accurate design while the PVA threads are still easy to remove.

### 4.3 Silicone Molding

We cast silicone over the embroidered substrate to create the silicone-textile composite. Double-sided tapes are used to tape down the top side of the substrate, i.e. the side with water-soluble thread, onto the bottom of the mold. We tape down the ends of conductive threads to avoid accidental insulation of the electrical connection ends. The molds are 3D printed with off-the-shelf PLA/ABS filaments on consumer-grade printers like Ultimaker 3. The molds are 0.7mm in depth unless otherwise specified in the paper. We mix Ecoflex 00-30 (SMOOTH-ON) in a 1:1 weight ratio and pour it over the taped-down substrate. The silicone surface is then leveled and smoothed using a spreader (Step 4 in Figure 4). After the silicone rubber cures, we wash the substrate under warm water to dissolve the water-soluble thread and remove the clear PVC layer (Step 5 in Figure 4). Then, the substrate is trimmed along the edges so that it could be placed back into the mold for the second layer of silicone casting (Step 6 in Figure 4). The conductive ends are taped down again, the same as the first layer of casting. The second layer of silicone fills up the holes that the water-soluble thread originally lied in. Once the second layer of silicone is cured, we brush a thin layer of silicone to adhere the adhesives: the skin-safe adhesive sheets from Sunnyscopa Printable Temporary Tattoo Paper.

## 5 CHARACTERIZATION: UNDERSTANDING SKINERGY SIGNALS

Our system measures the voltage difference across the load resistor that connects the TENG and the reference GND electrode to sense different touch-based interactions. We use rectifiers for the AC signals to be measurable by the microcontroller. Figure 6 shows the voltage profiles of the contact-separation and sliding mechanisms before and after rectifications. The measured voltage is upper-bounded by open-circuit voltage, $V_{oc}$. Open circuit voltage is the difference in electrical potential between two terminals (*e.g.*, TENG electrode and the reference electrode) when no load is connected. For small contact areas like the ones between the finger and the sensor, $V_{oc}$, can be given by [42]:

$$V_{oc} = \frac{\sigma}{2\epsilon_0} A \tag{1}$$

In this equation, $\sigma$ is the tribo charge density between skin and silicone, $\epsilon_0$ is the absolute permittivity constant of the dielectric, and $A$ is the area of the contact.

In this section, we characterize the impact of load resistance (Sec 5.1) and electrode shape (Sec 5.2) on generated voltages. We

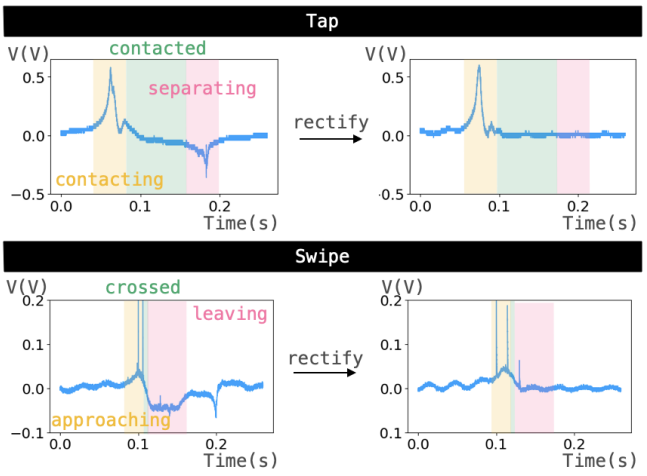


**Figure 6: Measured voltages of the contact-separation and sliding mechanisms before and after rectification.**

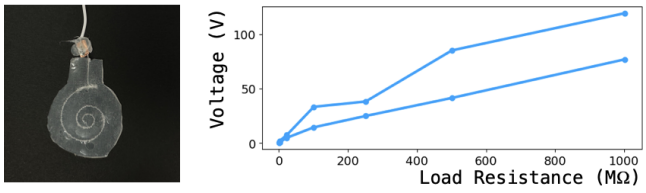


**Figure 7: The voltage increases as the load resistance increases. Left: the circular sensor (readius=1.5cm)used for the experiment. Right: The load resistance - voltage profile.**

then show the measured voltages are sensitive to pressure and spatiality (Sec 5.3). Finally, we evaluate the stretchability & repeatability (Sec 5.4) of Skinergy.

### 5.1 Load Resistance - Voltage Profile

The generated voltage depends on the load resistance due to the external resistance's limitation on the real charge transfer rate [43]. To characterize the impedance response of the sensor, we measure peak voltages generated from the tap motion when connected to varying load resistances. The exact resistance-voltage profile varies across users due to different tapping motions (*e.g.*, force, speed) and skin properties (*e.g.* skin hydration) affecting $\sigma$.

Figure 7 shows two resistance-voltage profiles from two people's tapping motions. The 0.7mm-thick prototype is adhered to the back of their left hand, rectified and connected to the oscilloscope (SIGLENT SDS 1202X-E) for measurements. To vary the load resistance, we connect resistors in series with the oscilloscope and calculate the voltage using Ohm's law. For each resistance value, they are instructed to try their best to tap at the center of the prototype ten times continuously and consistently. We record the peak voltage among all ten taps.

This experiment informed the load resistance selection in our customized sensing board. Note that when we use a microcontroller for TENG signals measurements, the overall load resistance is a

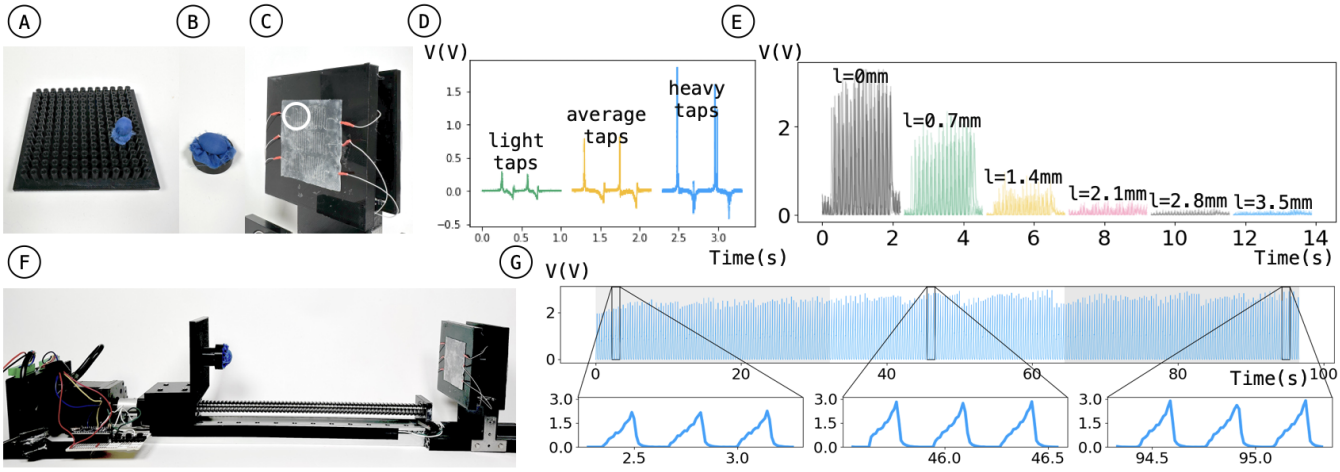


**Figure 8: (A) The indenter covered with Nylon for spatiality sensitivity experiment. (B) The indenter covered with Nylon for repeatability experiment. (C) The prototype for repeatability experiment. The white circle indicates the contact position. (D) Effect of force (0.05N, 0.3N, 1.4N) on measured voltages generated by two taps. (E) Spatiality Sensitivity Characterization. (F) Our customized testing rig is based on a linear stage actuator. Indenters (left) move along the axis to contact with and separate from the sensor (right). (G) Repeatability characterization. We use the customized testing rig to tap the sensor 300 times. We zoom in on contact-separation cycles at the beginning, middle, and end of the experiment.**

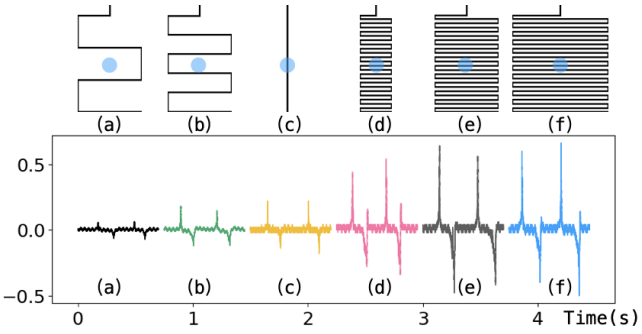


**Figure 9: Effect of electrode shape on measured voltages generated by two taps. Blue dots indicate tapping locations.**

complicated resistance network of all circuit components, in addition to the explicit load resistors, between the sensing electrode and the ground. Thus, when we use the same load resistance on the sensing board, the exact peak voltages vary, but the relative trend maintains.

## 5.2 Electrode Shape

Parallel placements of single-electrode mode TENG scale up $V_{oc}$ [42]. We fabricated six prototypes of the same size (60mm x 60 mm x 0.7mm) with different rectangular zigzag electrode shapes embroidered in the center. As shown in Figure 9, there are 3 spacing parameters: 2mm (d-f), 9mm (b), and 16mm (a). There are 4 width parameters: 0mm (c), 15mm (d), 30mm (a,b,e), and 45mm (f). The prototypes are directly connected to the oscilloscope for measurements using its internal impedance as the load resistance. We show voltages generated from two taps in the center for each shape.

Comparing (a), (b), and (e), we observed that a high proportion of conductive thread length over a given area correlates to a higher voltage output. Further, we observe that close proximity between the tap and the electrode correlates to higher output.

This experiment informed electrode shape and placement designs for different sensing applications.

## 5.3 Pressure & Spatiality Sensitivity

TENGs are force-sensitive because the tribo charge, $\sigma$, increases as contact pressure increases [36]. Figure 8D shows signals of finger taps with different forces on the same Skinergy prototype (Figure 9F), measured by oscilloscope loaded with its own impedance. Heavy taps correlate to signals with larger magnitudes.

Our thread-based TENGs have spatial sensitivity because the electrodes do not fully cover the dielectric layers. Because precisely controlling finger tap force, speed, and locations is difficult, we built a testing rig based on a linear stage actuator (Figure 8F). The rig allows easy control of indenter locations and consistently performs the contact-separation cycles. We cover the indenters with Nylon fabric, a positive triboelectric material.

Figure 8E shows that given the same tapping force, peak voltages decrease as the tap location moves further away from the electrode. For the experiment, we 3D printed an indenter base (Figure 8A) so that the small rounded indenter can move linearly with a step size of 7mm. We perform the contact-separation cycle 10 times continuously per session, and 5 sessions per location. The signals are measured with the same circuit as our customized sensing board (Section 6.1) which has a much larger load resistance than the oscilloscope. We plot all contact-separation cycles in the figure.

Pressure and spatiality sensitivities informed our algorithm designs. Because pressure and spatiality impact Skinergy signals, for localization tasks, we find it helpful to calculate the ratio of the

electrode signal over the sum of signals of all electrodes to remove the force factor.

### 5.4 Stretchability & Repeatability

Our silicone-textile composite sensors exhibit promising tensile capabilities for on-skin uses. We prepare three samples for tensile tests on Instron Universal Testing System (Instron 5566): a straight trace, a narrow zigzag trace, and a wide serpentine trace. All sensors remained intact until 150% elongation. We further test the sensor performance under strain, for the zigzag trace, the signals remained similar up to 60% elongation, consistent with prior works and beyond what human skin can endure.

To investigate the repeatability of Skinergy, we use the customized testing rig to perform contact-separation cycles 300 times: 3 sessions of 100 continuous cycles using an oval-shaped indenter (Figure 8A), similar to the shape of a finger. Figure 8G shows that the shapes of the signals remain consistent throughout the experiment. Moreover, we did not notice sensor performance degradation during the development process. Note that the perceived signal "drifting" is caused by force variations in the testing rig, a more in-depth repeatability finding can be found at [8].

## 6 SENSING INTERACTIONS

Skinergy senses interactions with a customized sensing board and different signal processing pipelines for different sensing tasks.

### 6.1 Customized Sensing Board

The customized sensing board is an experimental apparatus that serves as a proof-of-concept system implementation of Skinergy. The purpose of the board is to measure the electrical signals generated by gestural interactions and send the measured signals to a nearby computing device (*e.g.,* computers or smartphones) for signal processing. Typically, TENG's signals are measured by bulky, large and expensive instruments. The board costs around US$54, and could be significantly decreased when produced in bulk. The energy consumption of the board is 37mW.

*Mircrocontroller Unit.* The hub of the sensing board is XIAO nRF52840 (Seeed Studio), a microcontroller unit (MCU) incorporated with the Nordic nRF52840 chip (Nordic Semiconductor). The low-power MCU implements Bluetooth 5 and provides Bluetooth Low Energy (BLE) functions with an onboard antenna. The board is powered by a 3.7V, 190mAh Lipo Battery. A 3.3V voltage regulator provides a constant voltage source to the MCU. The MCU has 6 built-in analog I/O pins that allow reading up to 6 electrodes. The analog pins are multiplexed into the 12-bit analog-digital converter (ADC). We use Arduino for firmware programming and UART for BLE communication.

Note that even though there is a battery in our sensing board, it is used to power the readout circuit and wireless transmission. The sensor itself does not rely on the battery.

*Signal Acquisition.* The sensing board measures the voltage difference between the *sensor electrode*, the conductive thread embedded inside silicone, and the *reference electrode*, the ground (GND) of the MCU. TENG signals naturally have low currents, high voltages, and high input impedance. The generated voltages are easier

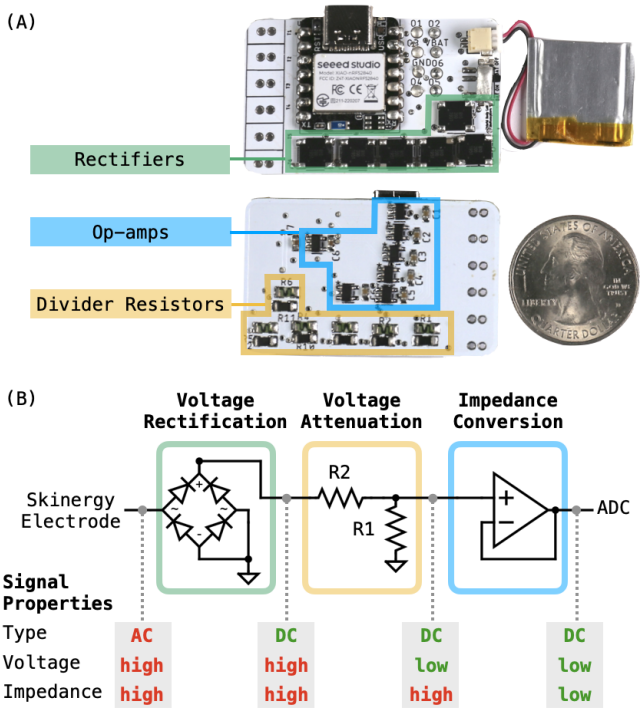


**Figure 10: PCB and the signal acquisition schematic. (A): Our custom untethered sensing board. (B): The signal acquisition circuit has 3 stages: (1) voltage rectification using full-bridge rectifiers, (2) voltage attenuation using divider resistors; and (3) impedance conversion using op-amps. The signal acquisition circuit converts high-voltage high-impedance AC voltages to low-voltage low-impedance DC voltages to be read by the microcontroller.**

to measure than the generated currents because the low-current signals require amplification. The signal magnitudes are affected by load resistances, characterized in Section 5.1. We implement the signal acquisition circuit proposed by Lu et al. [33] Each analog I/O pin has its own signal acquisition circuit. The circuit has 3 stages:

- Voltage Rectification Stage: We use full-bridge rectifiers (CDMBL102S) to convert the AC signals, generated by TENGs, into non-negative DC signals to satisfy the ADC range lower-bound requirement.
- Voltage Attenuation Stage: The load resistance for TENG is the sum of resistance values of R1 (200MΩ, Vishay Dale) and R2 (1GΩ, Vishay Dale). We use a passive voltage divider network of two resistors to reduce the magnitude of signals (i.e. only reading the voltage difference across R1) to satisfy the ADC range upper-bound requirement.
- Impedance Conversion Stage: We implement a voltage follower using a rail-to-rail op-amp (MCP6V81). The op-amp is powered by the regulated 3.3V supply, ensuring the output signal does not exceed 3.3V. The voltage follower converts high-impedance input signals into low-impedance input signals to satisfy ADC input impedance requirements.

*Data Acquisition.* For each reading frame, we read the 6 analog I/O pins sequentially with 2 milliseconds delay in between, resulting in a sampling rate of approximately 93 frames/second. Once we have the frame, we send the data to a nearby computer/smartphone via Bluetooth.

## 6.2 Electrode Placements & Data Processing Pipeline

The electrode placements are based on sensing applications. This section shows some example electrode placements and their associated sensing algorithms.

*6.2.1 Discrete Touch Detection.* Figure 6 shows the voltage profile of the contact-separation mechanism of a touch. Discrete touch inputs can be easily detected with a simple threshold. Figure 11A shows the sensor recognizing a discrete touch.

*6.2.2 Multi-contact Detection.* When more than one contact-separation occurs simultaneously, Skinergy is able to detect multiple contacts. The algorithm is the same as the discrete touch inputs with simple thresholding (Figure 11B).

*6.2.3 Contact Localization Matrix.* As shown in Figure 12, employing the matrix-style electrode placement, similar to that of the resistive matrix, Skinergy becomes a matrix capable of contact localization. The matrix design could be as simple as straight lines (Figure 12A). More complicated designs [48], like the one in Figure 12B, has better performance as it reduces crosstalk effects. For the 3x3 matrix examples, the reading at each intersection is calculated as the sum of signal readings from its vertical line and horizontal line.

*6.2.4 Gesture Recognition.* For gesture recognition tasks, we use a square patch with 6 rectangular electrodes with zigzag traces. As shown in Figure 13, the gestures have distinct signal profiles. For example, both pinch and spread start with sensor contacting, indicated by the middle yellow and gray peaks. A pinch pulls the skin away from the hand and triggers all other channels, but a spread triggers only the pink (top right) and black (bottom left) channels as fingers move diagonally.

To train and test the machine learning (ML) models, we input a 3-second window of all 6 continuously sampled channels. To better capture the temporal information, the 3-second window is further divided into 1.5s-long sliding windows with 50% overlapping. As mentioned in the characterization section, we found it helpful to consider the normalized signal: the ratio of the signal of a channel over the sum of all channels. In addition to the standard statistical features of both the original and normalized signals: mean & standard deviation (std), we use peak characteristics as rectified TENG signals form peaks in response to events (Figure 6). For each channel, we detect peaks using `find_peaks`[6]. Then, we calculate the following features on both the original signals and the normalized signals: argmax, the occurring order of argmax with respect to other channels, the number of peaks, the mean distance between the peaks, mean & std of peak prominences, and mean & std of peak heights. All of these features are aggregated and input into the respective `ExtraTreesClassifier`[7] for training and prediction.

[6]SciPy.Signal v1.10.1 with prominence=5, and height=0.1

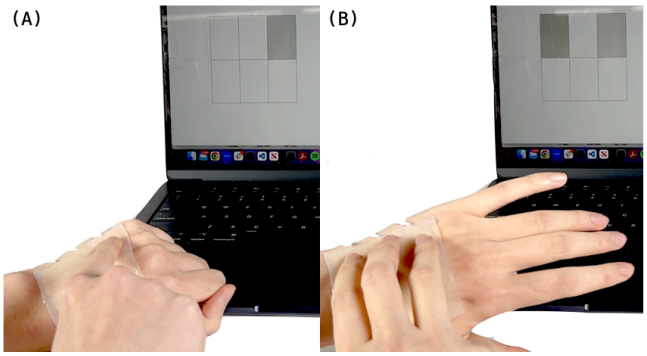


**Figure 11: (A): single touch detection. (B): multi-touches detection. The electrode design in both images is the same as the design in Figure 13.**

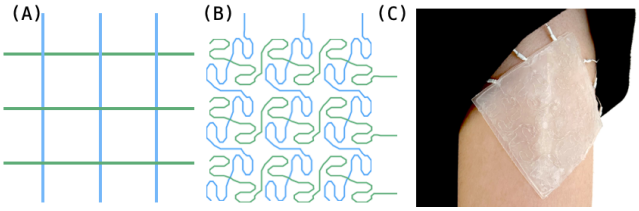


**Figure 12: (A): a simple matrix design; (B): a more optimized matrix design that minimizes cross-talking; (C): fabricated sensor of the optimized matrix design attached to the upper arm.**

# 7 USER STUDY

We conducted a user study to (a) evaluate Skinergy's gesture recognition performance, and (b) probe user perceptions and envisioned applications.

## 7.1 Method

The two main parts of study are the sensor data collection for machine learning (ML) model validation, and a semi-structured interview gauging user perceptions and envisioned applications.

*7.1.1 Participants & Apparatus.* We recruited ten participants (four male and six female, mean age=25.3) via word-of-mouth. All participants were right-handed. The participants were given US$15 Amazon gift cards as gratuities.

The experiment used an Apple Macbook Air (2022), and data was transmitted from the sensor board using Bluetooth. The sensing board is a customized PCB with the same circuit described in Section 6.1 but with a slightly different layout.

*7.1.2 Study Protocol.* Our study consisted of (1) a pre-study survey, (2) a sensor data collection process, (3) a post-usage survey, and (4) a semi-structured interview.

[7]Default sciki-learn(v1.2.2) parameters

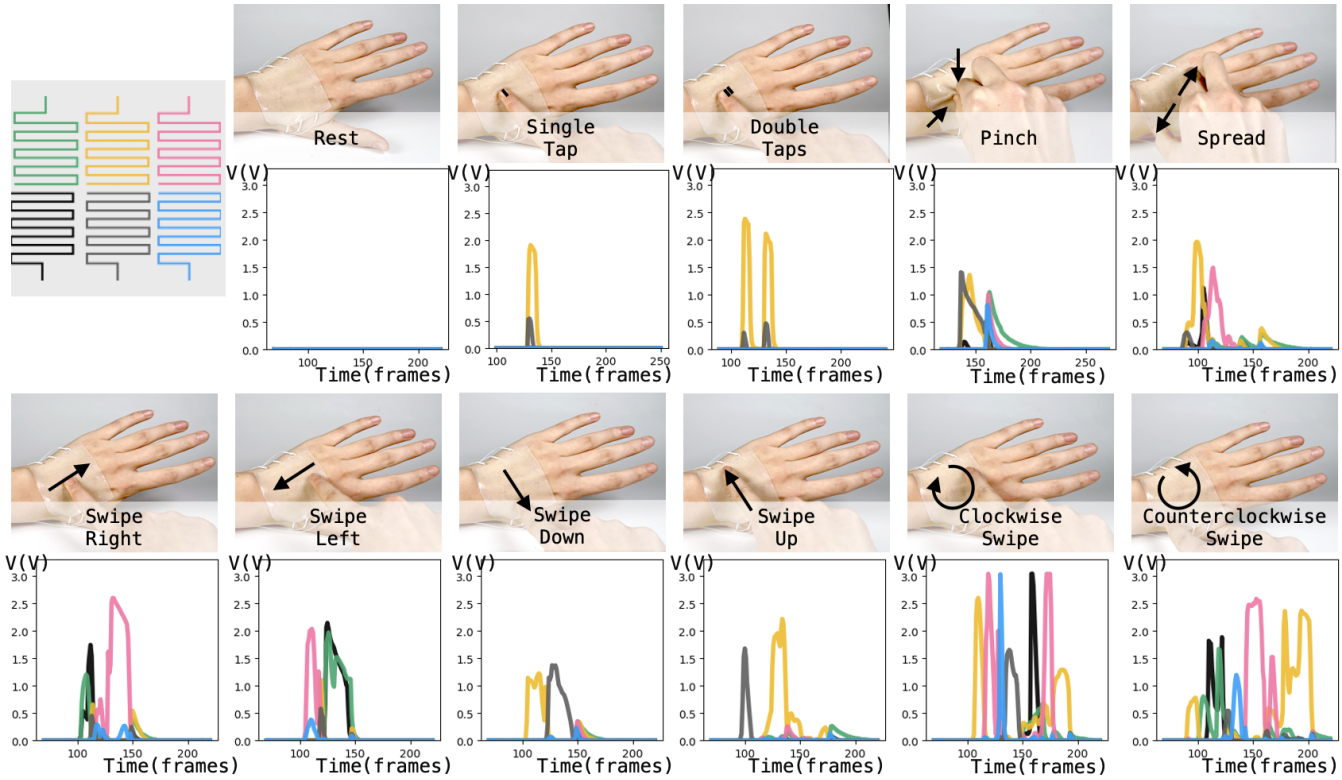


**Figure 13: Gestures and corresponding example signals. The top left is the electrode design of the sensor. Colors map the electrode to the signals generated from it.**

*(1) Pre-Study Survey (5 minutes).* Participants were asked to fill out the survey at the beginning of the study. The survey included a questionnaire regarding demographic data, experience with wearable devices, dominant hand, and if they self-identify that their hands sweat often.
*(2) Gesture Recognition Data Collection (20 minutes).* At the beginning of the study, an experimenter adhered the sensor to the back of their non-dominant hand, and the sensing circuit to their forearms (Figure 1). Each participant uses a new sensor. We first showed a brief demonstration of each gesture to the participants and the usage of the data collection system. Once the participant felt familiarized with the data collection system, data collection began. We generated a randomized order of ten trials of eleven gestures, and the participants performed them as called out. The participants heard instructions from the computer what gesture to perform and when to start/end the gesture. We recorded 3 seconds for each gesture, with the instruction beginning and ending at the 0.5- and 2.5-second points. The participants are seated with their non-dominant hands lying flat on a table throughout the study. A sheet of copy paper is placed under their hand to observe if their hands get sweaty. All participants were free to move between gestures. The device is removed after the collection process ends.
*(3) Post-Usage survey (5 minutes).* Participants were asked to fill out a post-usage survey after device removal. The survey included Likert Scale questions on device acceptability and comfort.
*(4) Semi-structured Interview (30 minutes).* The interview started by asking about their overall experience. The experimenter showed the participants images of look-alike prototypes with aesthetic designs attached to the skin. The experimenter followed up with questions regarding aesthetics, comparison with other technologies, and customization. Then, there was a 5-min sketching activity in which the participants were asked to sketch three sensor customizations. Finally, the experimenter asked about the participant's social perceptions, opinions on self-powered on-skin wearables, and envisioned applications. The interview was recorded, transcribed, and analyzed using the grounded theory approach [5].

## 7.2 Gesture Recognition

For the gesture recognition study, we chose 11 gestures (see the full list in Figure 13). These 11 gestures include a "rest" class, a no gesture-state, to detect whether touch inputs occurred.

*7.2.1 Results.* For the 11-class gesture recognition task, we achieved 92.8% accuracy for a within-user model using the leave-one-trial-out cross-validation and 79.7% accuracy trained an across-user model using the leave-one-participant-out cross-validation. The confusion matrices are shown in Figure 14. For both models, all "rest", the no gesture-state, are correctly predicted.

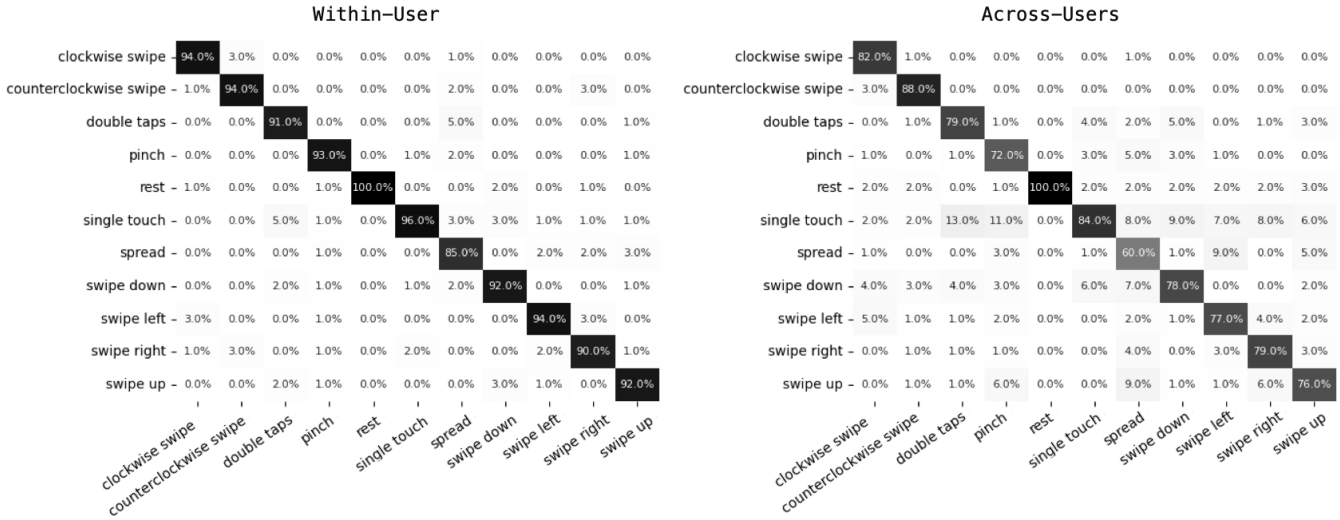


**Figure 14: Confusion matrices of 11-class gesture recognition. Within-user cross-validation (left) achieves 92.8% and across-user cross-validation (right) achieves 79.7%.**

*7.2.2 Discussion.* This study demonstrated gesture recognition feasibility at the back of the hand. The within-user accuracy suggests that gestures can be detected with high accuracy for every sensor attachment session. The across-user accuracy indicates that even for different sensors attached to different users, the algorithm still generalizes, meaning our fabrication approach has high reproducibility. The lower cross-user accuracy is attributed to individual skin differences and a lack of training data.

We observed noticeable differences between participants with sweaty hands (either self-reported or the printing paper underneath their hand was fully soaked after the study) and those with drier hands. The former (sweaty hands) yields a within-user mean accuracy of 85.0%, while the latter (non-sweaty hands) achieves a within-user mean accuracy of 94.5%. This difference further affects the cross-user performance, even though alleviated with the normalized signals. The sensor signals have larger amplitudes with drier fingers. High-amplitude gestures from sweaty fingers are confused with low-amplitude gestures from dry fingers.

Our finding suggests that for robust gesture detection, pretrained ML models need to consider individual differences like skin properties. Further, increasing the amount of training data will also increase the cross-user performance and remains integral future work.

## 7.3 Qualitative Analysis

Most participants found the try-on prototype to be appealing to wear (Median (M)=5 on the Likert scale; 1=strongly disagree, 7=strongly agree) and could see themselves wearing the device (Median (M)=5 on the Likert scale; 1=strongly disagree, 7=strongly agree). U7 and U8 described Skinergy like "cyberpunk". U8 found it cool that "the device totally [is] like together with my human body". We summarize our findings into the following five themes.

*7.3.1 Self-powered On-skin Sensors.* All but one participant had immediate positive reactions towards self-powered on-skin sensors: "convenient" (Number of participants (N)=3), "cool" (N=3), "impressive" (N=1), "good" (N=1), "necessary" (N=1), and "a very big aspect" (N=1). The other participant (P4) believes it *"depends on how much energy it can save."* Battery life is a common consideration when choosing wearable devices in general (N=6). Charging the device less often or not needing to charge at all makes a difference in using the device. U1 mentioned the emergency situation: *"if you have some emergency...but [the device] is out of battery, it is a very bad case"*. U3 found the silicone-textile composite of the prototype to be "very useful" but wished our proof-of-concept sensing board and the battery could also be miniaturized to a skin form. Other participants echoed that removing the battery would make the system significantly smaller (N=4), softer (N=3), and lighter (N=2) compared to the current prototype they experienced. Three participants believed that self-powered sensors contribute positively to sustainability. U4 states that *"convert[ing] energy from someone's body to power a device is good for the Earth."* U7 also pointed out that *"lithium batteries are very bad for the planet."*

*7.3.2 Envisioned Applications.* An always-available easy-to-access remote control is the most popular envisioned application (N=9), examples including a music/video player (N=5), a game controller (N=3) for "deep immersion" (U10), controlling home appliances with "a tap on your hand" (U1), remotely locking/unlocking the car so that they do not need to look for the key (U2), unlocking the door with a magic pattern (U7), picking up calls (U3), etc. U7 pointed out that our interface is *"better for actions when [they] don't need or don't want to see the screen"* of their smartphones. There is also interest in the passive harvesting of biomechanical energy, including fitness tracking (N=4) and sleep movement monitoring (N=1), because users then *"don't need to touch stuff"* (U5). U1 and U3 found Skinergy suitable for emergency situation notification systems with immediate and subtle actions. Although our sensors

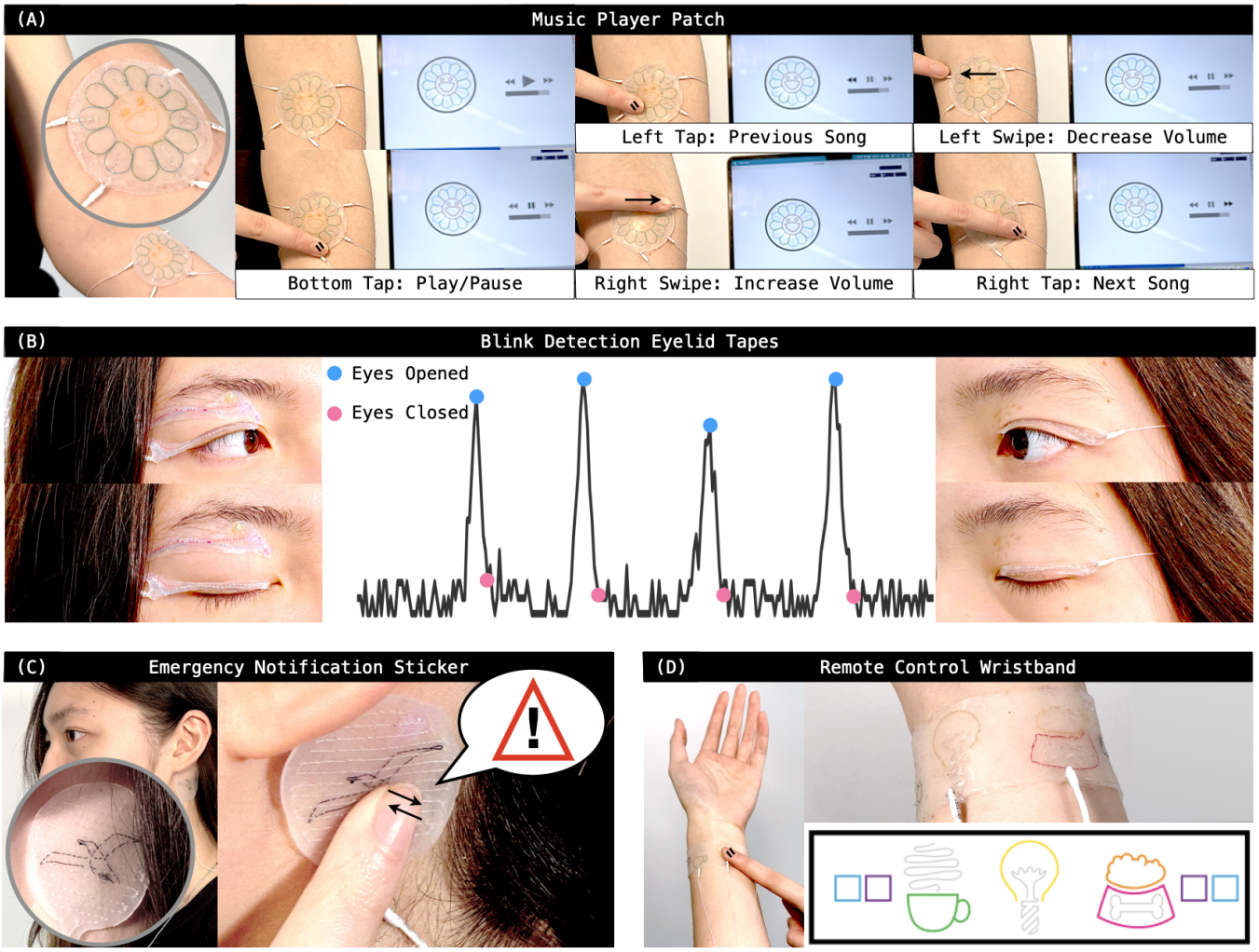


**Figure 15: Example applications. (A) A forearm music player patch inspired by Takashi Murakami's flowers. (B) Discrete (right) and decorative(left) eyelid tapes that detect eye blinks. The visualized signals show that mechanical movements of the eyelids generate measurable electrical signals. (C) A behind-the-ear sticker for sending emergency notifications. (D) A wristband for remotely controlling home appliances.**

do not yet have the envisioned functionalities, participants envisioned applications such as physiological tracking (N=3), medical uses (N=2), and wearable reminders (N=2).

*7.3.3 Customizability.* Functionality and aesthetic customizability coincide for Skinergy. Aesthetic designs are perceived as "a form of expression" (U2) and "a fashion statement" (U6). Some participants (N=2) suggested visual designs (colors and patterns) could indicate functionality. U5 sketched sensor electrode placements as part of the icon designs for the corresponding function, which we implemented in our remote control application (see Section 8). Interestingly, U5 valued aesthetics over functionality, yet U3 and U8 valued functionality over aesthetics. Other individual differences lie in acceptable or preferred worn locations. Some (N=2) want their sensors to be obvious: *"It has to show; otherwise, what's the point of this aesthetic design?"* (U6). Others (N=3) want their sensors to be "invisible," "as discreet as possible," and "as small as possible"(U2). These findings highlight the importance of customization, echoing findings of other on-skin work [21]. U10 suggested the "functional parts" could be the same every day, but the "decoration" can be changed daily based on the outfits. Customization is further demanded by different contexts like formal/informal events (U2, U3, U9) and seasons (U10).

*7.3.4 Comparison with Existing Wearable Forms.* Participants compared Skinergy with temporary tattoos (N=10) and found Skinergy to remind them of smartphones (N=8) and smartwatches (N=5). Our sensors are found to be thicker (N=4) and more inhibiting (N=3) than temporary tattoos, but they are deemed more useful (N=2) for their sensing capabilities. U2 would like Skinergy to be "as indistinguishable as temporary tattoos" like "transparent pimple stickers". U6 and U7 wish for on-skin sensors to have visual designs similar to

their desired tattoo designs. When compared with other computing devices like smartphones and smartwatches, convenience is the main advantage (N=5). U1 pointed out that with a smartphone, they still "need to find out where the app is," but an on-skin interface is always available. When compared with other wearable devices, i.e. smartwatches, Skinergy is deemed lighter (U1, U2), more accurate at physiological tracking/monitoring (U6), and more comfortable, as U8 and U9 do not like wearing things on their wrists.

*7.3.5 Areas of Concern.* The main concern amongst participants is the skin adhesive (N=7). Most of the participants found the application process comfortable (Median (M)=6 on the Likert scale; 1=strongly disagree, 7=strongly agree) but the removal uncomfortable (Median (M)=3 on the Likert scale; 1=strongly disagree, 7=strongly agree). Removing Skinergy was uncomfortable because prototypes were only worn for approximately 20 minutes during the study. When the devices were removed, they were still sticky, and adhesive residue remained on the skin. In terms of functionalities, Some participants expressed the need for feedback/output modalities (N=4). U6 noted that "if [Skinergy] has a screen, [they] will definitely use it." Participants were concerned about the sensing board and wires coming out of the sensor (N=4) and envisioned the device to be "just the patch" (U5). Other observed concerns include reusability (N=3) and durability (N=2).

## 8 APPLICATIONS

We implemented real-time sensing systems to demonstrate Skinergy's potential as an on-skin sensor when placed on different body parts (Figure 15).

*Behind-the-Ear Sticker: Emergency Notification System.* Skinergy can take the form of a small and discreet sticker behind the ear that sends emergency notifications when the user feels in danger (Figure 15C). The sensor can be activated by stroking the sticker. The small form factor, discreet body location, subtle gesture for activation, and long battery life enabled by the self-powered sensor offer the user a tool to quickly and inconspinuously call for help without aggravating the situation.

*Eyelid Tapes: Blink Detection.* Skinergy serves as a blink detector when it is in the shape of an eyelid tape and adhered to the top eyelid (Figure 15B). The visual design can be either discrete or expressive, depending on user preferences. The natural blinking motions perform contact-separation cycles between the sensor and the eyelid. The measured signals show clear peaks that correspond to eye openings. This passive sensing application highlights Skinergy's potential for usage without explicit human inputs.

*Wristband: Remote Control.* Skinergy can be used as an on-the-body remote control (Figure 15D). Here we demonstrate its use as (a) a coffee maker activator, (b) a light switch, and (c) a dog feeder. The wristband form factor affords accessible and always-available interactions. Each function is created as a distinct button that is triggered by tapping on the corresponding sensor. Note that the electrode shape of the gray sensing lines is a part of the icons, as suggested by our participant.

*Inner-Forearm Patch: Music Player.* For the inner-forearm patch music player (Figure 15D), we implemented real-time predictors using the ML model described in Section 6.2.4. The live predictor takes the latest 3 seconds of data as input to the trained model and continuously predicts the gestures. The gestures we used are: bottom tap → play/pause; left swipe → decrease volume; left tap → previous song; right swipe → increase volume; right tap → next song. Although we placed the patch on the inner forearm, users can place it anywhere on-body that they would like. The electrode placement of the flower design is very different from that of the user study prototype, showing a high degree of customizability.

## 9 DISCUSSION, LIMITATIONS AND FUTURE WORK

**Towards Fully Self-Powered Devices.** In this paper, we explored TENGs' self-powered wearable sensing capabilities, but the generated energy could be harvested to (a) either power other circuit components *instantaneously* or (b) stored with a supercapacitor to provide streamed electrical power for later uses [54]. TENG is not the only self-powered sensing technique [7, 44, 61] and recent works further shed light on flexible energy-storage units[30]. The device itself could be self-sustained, alleviating the need for bulky and rigid components in wearable systems and filling the gap between portable and distributed powering solutions demanded by the rise of ubiquitous computing.

**Understanding Individual Skin Properties.** Throughout our development process, we observed noticeable differences in signals induced by dry and sweaty fingers: dryer skins have higher peak voltages. Our quantitative user studies also support the observation. This is most likely related to $\sigma$, the tribo charge density term in Equation 1. There could be other factors that are harder to notice. For example, female dermal dielectric constant values are observed to be on an average 9% higher compared with respective male skin [39]. A systematic evaluation of how skin properties are related to skin-based TENG performances is indispensable for robust and generalized sensing and energy harvesting usages.

**Electrode Design and Placement.** The electrode designs in our prototypes are informed by the characterization experiments but could be further optimized. Different sensing applications have different design requirements. For example, a matrix-style contact localization sensor desires minimal crosstalks, so the electrode design benefits from a sparse distribution. In contrast, for a gesture recognition sensor, like the one used in the user studies, the "crosstalks" are useful signals for spatial information. Electrode design and placement also need to be considered for embroidability. If the spacing between the electrode traces is too small, the stabilizers are difficult or impossible to tear. Our experiment with wash-away PVA stabilizers showed that the large amount of dissolved PVA gets absorbed by the conductive threads, making them stiff. This poses a limitation of our fabrication method. Our electrode design can only be traces with sufficient spacings (around 1mm) in between. Future works on optimized electrode design and placement motivated by sensing applications will improve sensing performances.

**Towards Scalable Manufacture.** Depending on the complexity of the design, the entire fabrication process of Skinergy for each sensor takes around 8.55 hours, 8 of which is dedicated to curing silicone. Approximately, embroidery (Step 1-3 in Figure 4) takes 0.25h. Silicone molding (Step 4-6 in Figure 4) takes 8.2h: 0.2h working time

and 8h curing time. Multiple sensors can be batched to reduce curing time: batching 10 devices together will take 5.5h working time and 8h curing time. The fabrication time can be further minimized with larger batches, larger embroidery machine working areas (10.16 x 10.16cm in our home embroidery machine), and commercial embroidery machines for scalable and inexpensive on-skin devices. Machine embroidery has benefits over other fabrication methods as it increases durability & reproducibility and lowers complexity, but it is worthwhile to consider other scalable fabrication methods: 2D printing [32], laser-cutting for flexible sensing [13, 37], 3D printing directly into semi-fluid solutions [37], 3D printing channels [64, 70], threading in materials as a post-process [52], customizing jigs [56] like the ones in [8], and spraying conductive materials [65]. Finally, future work could develop simulation features based on the digital fabrication methods [16, 50, 58].

## 10 CONCLUSION

In this work, we propose Skinergy, self-powered on-skin gesture sensors. The silicone-textile composite sensors are fabricated with off-the-shelf materials and readily-available processes. The self-powered sensing is enabled by the Triboelectric Nanogenerators (TENGs) phenomenons. We demonstrated a diverse set of sensing tasks. Our sensor design allows versatile designs in terms of both functionalities and aesthetics. Skinergy tackles self-powered on-skin sensors towards wider, real-world adoption of on-skin devices.

## ACKNOWLEDGMENTS

This project was supported by the National Science Foundation under Grant IIS-2047249 and Cornell Atkinson Center for Sustainability. We thank Chi-Jung Lee, Jingwen Zhu, Pin-Sung Ku, and Heather Kim for their inputs, and Xia Zeng and Charles V. Beach, Jr. for the technical support. We also would like to thank the study participants and the reviewers.

## REFERENCES

[1] Roland Aigner, Andreas Pointner, Thomas Preindl, Rainer Danner, and Michael Haller. 2021. TexYZ: Embroidering Enameled Wires for Three Degree-of-Freedom Mutual Capacitive Sensing. In *Proceedings of the 2021 CHI Conference on Human Factors in Computing Systems*. 1–12.

[2] Roland Aigner, Andreas Pointner, Thomas Preindl, Patrick Parzer, and Michael Haller. 2020. Embroidered resistive pressure sensors: A novel approach for textile interfaces. In *Proceedings of the 2020 CHI Conference on Human Factors in Computing Systems*. 1–13.

[3] Nivedita Arora, Steven L Zhang, Fereshteh Shahmiri, Diego Osorio, Yi-Cheng Wang, Mohit Gupta, Zhengjun Wang, Thad Starner, Zhong Lin Wang, and Gregory D Abowd. 2018. SATURN: A thin and flexible self-powered microphone leveraging triboelectric nanogenerator. *Proceedings of the ACM on Interactive, Mobile, Wearable and Ubiquitous Technologies* 2, 2 (2018), 1–28.

[4] Joanna Berzowska, Alex Mommersteeg, Laura Isabel Rosero Grueso, Eric Ducray, Michael Patrick Rabo, and Geneviève Moisan. 2019. Baby Tango: electronic textile toys for full-body interaction. In *Proceedings of the Thirteenth International Conference on Tangible, Embedded, and Embodied Interaction*. 437–442.

[5] Kathy Charmaz. 2006. *Constructing Grounded Theory*. Sage Publications, London, UK.

[6] Christopher Chen, David Howard, Steven L Zhang, Youngwook Do, Sienna Sun, Tingyu Cheng, Zhong Lin Wang, Gregory D Abowd, and HyunJoo Oh. 2020. SPIN (self-powered paper interfaces) bridging triboelectric nanogenerator with folding paper creases. In *Proceedings of the Fourteenth International Conference on Tangible, Embedded, and Embodied Interaction*. 431–442.

[7] Kai Dong, Xiao Peng, and Zhong Lin Wang. 2020. Fiber/fabric-based piezoelectric and triboelectric nanogenerators for flexible/stretchable and wearable electronics and artificial intelligence. *Advanced Materials* 32, 5 (2020), 1902549.

[8] Kai Dong, Zhiyi Wu, Jianan Deng, Aurelia C Wang, Haiyang Zou, Chaoyu Chen, Dongmei Hu, Bohong Gu, Baozhong Sun, and Zhong Lin Wang. 2018. A stretchable yarn embedded triboelectric nanogenerator as electronic skin for biomechanical energy harvesting and multifunctional pressure sensing. *Advanced Materials* 30, 43 (2018), 1804944.

[9] Shreyosi Endow, Mohammad Abu Nasir Rakib, Anvay Srivastava, Sara Rastegarpouyani, and Cesar Torres. 2022. Embr: A Creative Framework for Hand Embroidered Liquid Crystal Textile Displays. In *Proceedings of the 2022 CHI Conference on Human Factors in Computing Systems*. 1–14.

[10] Feng-Ru Fan, Zhong-Qun Tian, and Zhong Lin Wang. 2012. Flexible triboelectric generator. *Nano energy* 1, 2 (2012), 328–334.

[11] Maas Goudswaard, Abel Abraham, Bruna Goveia da Rocha, Kristina Andersen, and Rong-Hao Liang. 2020. FabriClick: interweaving pushbuttons into fabrics using 3D printing and digital embroidery. In *Proceedings of the 2020 ACM designing interactive systems conference*. 379–393.

[12] Bruna Goveia da Rocha, Oscar Tomico, Panos Markopoulos, and Daniel Tetteroo. 2020. Crafting Research Products through Digital Machine Embroidery. In *Proceedings of the 2020 ACM Designing Interactive Systems Conference*. 341–350.

[13] Daniel Groeger and Jürgen Steimle. 2019. Lasec: Instant fabrication of stretchable circuits using a laser cutter. In *Proceedings of the 2019 CHI Conference on Human Factors in Computing Systems*. 1–14.

[14] Nur Al-huda Hamdan, Simon Voelker, and Jan Borchers. 2018. Sketch&stitch: Interactive embroidery for e-textiles. In *Proceedings of the 2018 CHI Conference on Human Factors in Computing Systems*. 1–13.

[15] Nur Al-huda Hamdan, Adrian Wagner, Simon Voelker, Jürgen Steimle, and Jan Borchers. 2019. Springlets: Expressive, flexible and silent on-skin tactile interfaces. In *Proceedings of the 2019 CHI Conference on Human Factors in Computing Systems*. 1–14.

[16] Liang He, Xia Su, Huaishu Peng, Jeffrey Ian Lipton, and Jon E Froehlich. 2022. Kinergy: Creating 3D Printable Motion using Embedded Kinetic Energy. In *Proceedings of the 35th Annual ACM Symposium on User Interface Software and Technology*. 1–15.

[17] Kunpeng Huang, Ruojia Sun, Ximeng Zhang, Md Tahmidul Islam Molla, Margaret Dunne, Francois Guimbretiere, and Cindy Hsin-Liu Kao. 2021. WovenProbe: probing possibilities for weaving fully-integrated on-skin systems deployable in the field. In *Designing Interactive Systems Conference 2021*. 1143–1158.

[18] Jeyeon Jo and Cindy Hsin-Liu Kao. 2021. SkinLace: Freestanding Lace by Machine Embroidery for On-Skin Interface. In *Extended Abstracts of the 2021 CHI Conference on Human Factors in Computing Systems*. 1–6.

[19] Lee Jones and Sara Nabil. 2022. Goldwork Embroidery: Interviews with Practitioners on Working with Metal Threads and Opportunities for E-textile Hybrid Crafts. In *Creativity and Cognition*. 364–379.

[20] Hsin-Liu Kao, Artem Dementyev, Joseph A Paradiso, and Chris Schmandt. 2015. NailO: fingernails as an input surface. In *Proceedings of the 33rd Annual ACM Conference on Human Factors in Computing Systems*. 3015–3018.

[21] Hsin-Liu Kao, Christian Holz, Asta Roseway, Andres Calvo, and Chris Schmandt. 2016. DuoSkin: rapidly prototyping on-skin user interfaces using skin-friendly materials. In *Proceedings of the 2016 ACM International Symposium on Wearable Computers*. 16–23.

[22] Hsin-Liu Cindy Kao, Abdelkareem Bedri, and Kent Lyons. 2018. SkinWire: Fabricating a self-contained on-skin PCB for the hand. *Proceedings of the ACM on Interactive, Mobile, Wearable and Ubiquitous Technologies* 2, 3 (2018), 1–23.

[23] Mustafa Emre Karagozler, Ivan Poupyrev, Gary K Fedder, and Yuri Suzuki. 2013. Paper generators: harvesting energy from touching, rubbing and sliding. In *Proceedings of the 26th annual ACM symposium on User interface software and technology*. 23–30.

[24] Ali Kiaghadi, Morgan Baima, Jeremy Gummeson, Trisha Andrew, and Deepak Ganesan. 2018. Fabric as a sensor: Towards unobtrusive sensing of human behavior with triboelectric textiles. In *Proceedings of the 16th ACM Conference on Embedded Networked Sensor Systems*. 199–210.

[25] Dae-Hyeong Kim, Nanshu Lu, Rui Ma, Yun-Soung Kim, Rak-Hwan Kim, Shuodao Wang, Jian Wu, Sang Min Won, Hu Tao, Ahmad Islam, et al. 2011. Epidermal electronics. *science* 333, 6044 (2011), 838–843.

[26] Jin Hee Kim, Kunpeng Huang, Simone White, Melissa Conroy, and Cindy Hsin-Liu Kao. 2021. KnitDermis: Fabricating tactile on-body interfaces through machine knitting. In *Designing Interactive Systems Conference 2021*. 1183–1200.

[27] DoYoung Lee, SooHwan Lee, and Ian Oakley. 2020. Nailz: Sensing hand input with touch sensitive nails. In *Proceedings of the 2020 CHI Conference on Human Factors in Computing Systems*. 1–13.

[28] Yi-Chin Lee and Lea Albaugh. 2021. Hybrid embroidery games: Playing with materials, machines, and people. In *Designing Interactive Systems Conference 2021*. 749–762.

[29] Rongzhou Lin, Han-Joon Kim, Sippanat Achavananthadith, Ze Xiong, Jason KW Lee, Yong Lin Kong, and John S Ho. 2022. Digitally-embroidered liquid metal electronic textiles for wearable wireless systems. *Nature Communications* 13, 1 (2022), 2190.

[30] Ruiyuan Liu, Zhong Lin Wang, Kenjiro Fukuda, and Takao Someya. 2022. Flexible self-charging power sources. *Nature Reviews Materials* (2022), 1–17.

[31] Xin Liu, Bo Han, Clement Zheng, and Ching Chiuan Yen. 2022. Tribo Tribe: Triboelectric Interaction Sensing with 3D Physical Interfaces. In *CHI Conference on Human Factors in Computing Systems Extended Abstracts*. 1–6.

[32] Joanne Lo, Doris Jung Lin Lee, Nathan Wong, David Bui, and Eric Paulos. 2016. Skintillates: Designing and creating epidermal interactions. In *Proceedings of the 2016 ACM Conference on Designing Interactive Systems*. 853–864.

[33] Shan Lu, Wenqian Lei, Lingxiao Gao, Xin Chen, Daqiao Tong, Pengfei Yuan, Xiaojing Mu, and Hua Yu. 2021. Regulating the high-voltage and high-impedance characteristics of triboelectric nanogenerator toward practical self-powered sensors. *Nano Energy* 87 (2021), 106137.

[34] Elle Luo, Ruixuan Fu, Alicia Chu, Katia Vega, and Hsin-Liu Kao. 2020. Eslucent: an eyelid interface for detecting eye blinking. In *Proceedings of the 2020 International Symposium on Wearable Computers*. 58–62.

[35] Eric Markvicka, Guanyun Wang, Yi-Chin Lee, Gierad Laput, Carmel Majidi, and Lining Yao. 2019. Electrodermis: Fully untethered, stretchable, and highly-customizable electronic bandages. In *Proceedings of the 2019 CHI Conference on Human Factors in Computing Systems*. 1–10.

[36] Guanbo Min, Yang Xu, Peter Cochran, Nikolaj Gadegaard, Daniel M Mulvihill, and Ravinder Dahiya. 2021. Origin of the contact force-dependent response of triboelectric nanogenerators. *Nano Energy* 83 (2021), 105829.

[37] Hila Mor, Tianyu Yu, Ken Nakagaki, Benjamin Harvey Miller, Yichen Jia, and Hiroshi Ishii. 2020. Venous Materials: Towards Interactive Fluidic Mechanisms. In *Proceedings of the 2020 CHI Conference on Human Factors in Computing Systems*. 1–14.

[38] Sara Nabil, Jan Kučera, Nikoletta Karastathi, David S Kirk, and Peter Wright. 2019. Seamless seams: Crafting techniques for embedding fabrics with interactive actuation. In *Proceedings of the 2019 on Designing Interactive Systems Conference*. 987–999.

[39] Syed Akbar Raza Naqvi, Mohamed Manoufali, Beadaa Mohammed, Ahmed Toaha Mobashsher, Damien Foong, and Amin M Abbosh. 2020. In vivo human skin dielectric properties characterization and statistical analysis at frequencies from 1 to 30 GHz. *IEEE Transactions on Instrumentation and Measurement* 70 (2020), 1–10.

[40] Aditya Shekhar Nittala, Arshad Khan, Klaus Kruttwig, Tobias Kraus, and Jürgen Steimle. 2020. PhysioSkin: rapid fabrication of skin-conformal physiological interfaces. In *Proceedings of the 2020 CHI Conference on Human Factors in Computing Systems*. 1–10.

[41] Aditya Shekhar Nittala, Anusha Withana, Narjes Pourjafarian, and Jürgen Steimle. 2018. Multi-touch skin: A thin and flexible multi-touch sensor for on-skin input. In *Proceedings of the 2018 CHI Conference on Human Factors in Computing Systems*. 1–12.

[42] Simiao Niu, Ying Liu, Sihong Wang, Long Lin, Yu Sheng Zhou, Youfan Hu, and Zhong Lin Wang. 2014. Theoretical investigation and structural optimization of single-electrode triboelectric nanogenerators. *Advanced Functional Materials* 24, 22 (2014), 3332–3340.

[43] Simiao Niu, Sihong Wang, Long Lin, Ying Liu, Yu Sheng Zhou, Youfan Hu, and Zhong Lin Wang. 2013. Theoretical study of contact-mode triboelectric nanogenerators as an effective power source. *Energy & Environmental Science* 6, 12 (2013), 3576–3583.

[44] Joseph A Paradiso. 2006. Systems for human-powered mobile computing. In *Proceedings of the 43rd annual Design Automation Conference*. 645–650.

[45] Ernest Rehmatulla Post, Maggie Orth, Peter R Russo, and Neil Gershenfeld. 2000. E-broidery: Design and fabrication of textile-based computing. *IBM Systems journal* 39, 3.4 (2000), 840–860.

[46] Thomas Preindl, Cedric Honnet, Andreas Pointner, Roland Aigner, Joseph A Paradiso, and Michael Haller. 2020. Sonoflex: Embroidered speakers without permanent magnets. In *Proceedings of the 33rd Annual ACM Symposium on User Interface Software and Technology*. 675–685.

[47] Tarl W Prow, Jeffrey E Grice, Lynlee L Lin, Rokhaya Faye, Margaret Butler, Wolfgang Becker, Elisabeth MT Wurm, Corinne Yoong, Thomas A Robertson, H Peter Soyer, et al. 2011. Nanoparticles and microparticles for skin drug delivery. *Advanced drug delivery reviews* 63, 6 (2011), 470–491.

[48] Xianjie Pu, Qian Tang, Wensuo Chen, Zhengyong Huang, Guanlin Liu, Qixuan Zeng, Jie Chen, Hengyu Guo, Liming Xin, and Chenguo Hu. 2020. Flexible triboelectric 3D touch pad with unit subdivision structure for effective XY positioning and pressure sensing. *Nano Energy* 76 (2020), 105047.

[49] Tobias Röddiger, Michael Beigl, Daniel Wolffram, Matthias Budde, and Hongye Sun. 2020. PDMSkin: On-Skin Gestures with Printable Ultra-Stretchable Soft Electronic Second Skin. In *Proceedings of the Augmented Humans International Conference*. 1–9.

[50] Thijs Roumen, Ingo Apel, Jotaro Shigeyama, Abdullah Muhammad, and Patrick Baudisch. 2020. Kerf-canceling mechanisms: making laser-cut mechanisms operate across different laser cutters. In *Proceedings of the 33rd Annual ACM Symposium on User Interface Software and Technology*. 293–303.

[51] Marina Sala de Medeiros, Daniela Chanci, Carolina Moreno, Debkalpa Goswami, and Ramses V Martinez. 2019. Waterproof, breathable, and antibacterial self-powered e-textiles based on omniphobic triboelectric nanogenerators. *Advanced Functional Materials* 29, 42 (2019), 1904350.

[52] Valkyrie Savage, Ryan Schmidt, Tovi Grossman, George Fitzmaurice, and Björn Hartmann. 2014. A series of tubes: adding interactivity to 3D prints using internal pipes. In *Proceedings of the 27th annual ACM symposium on User interface software and technology*. 3–12.

[53] Fereshteh Shahmiri, Chaoyu Chen, Anandghan Waghmare, Dingtian Zhang, Shivan Mittal, Steven L Zhang, Yi-Cheng Wang, Zhong Lin Wang, Thad E Starner, and Gregory D Abowd. 2019. Serpentine: A self-powered reversibly deformable cord sensor for human input. In *Proceedings of the 2019 CHI Conference on Human Factors in Computing Systems*. 1–14.

[54] Yu Song, Jihong Min, You Yu, Haobin Wang, Yiran Yang, Haixia Zhang, and Wei Gao. 2020. Wireless battery-free wearable sweat sensor powered by human motion. *Science advances* 6, 40 (2020), eaay9842.

[55] Paul Strohmeier, Narjes Pourjafarian, Marion Koelle, Cedric Honnet, Bruno Fruchard, and Jürgen Steimle. 2020. Sketching on-body interactions using piezoresistive kinesiology tape. In *Proceedings of the Augmented Humans International Conference*. 1–7.

[56] Cesar Torres, Wilmot Li, and Eric Paulos. 2016. ProxyPrint: Supporting crafting practice through physical computational proxies. In *Proceedings of the 2016 ACM Conference on Designing Interactive Systems*. 158–169.

[57] Chonghe Wang, Xiaoyu Chen, Liu Wang, Mitsutoshi Makihata, Hsiao-Chuan Liu, Tao Zhou, and Xuanhe Zhao. 2022. Bioadhesive ultrasound for long-term continuous imaging of diverse organs. *Science* 377, 6605 (2022), 517–523.

[58] Guanyun Wang, Ye Tao, Ozguc Bertug Capunaman, Humphrey Yang, and Lining Yao. 2019. A-line: 4D printing morphing linear composite structures. In *Proceedings of the 2019 CHI Conference on Human Factors in Computing Systems*. 1–12.

[59] Yan Wang, Sunghoon Lee, Tomoyuki Yokota, Haoyang Wang, Zhi Jiang, Jiabin Wang, Mari Koizumi, and Takao Someya. 2020. A durable nanomesh on-skin strain gauge for natural skin motion monitoring with minimum mechanical constraints. *Science advances* 6, 33 (2020), eabb7043.

[60] Yanan Wang, Shijian Luo, Yujia Lu, Hebo Gong, Yexing Zhou, Shuai Liu, and Preben Hansen. 2017. AnimSkin: fabricating epidermis with interactive, functional and aesthetic color animation. In *Proceedings of the 2017 Conference on Designing Interactive Systems*. 397–401.

[61] Yinli Wang, Yaonan Yu, Xueyong Wei, and Fumio Narita. 2022. Self-powered wearable piezoelectric monitoring of human motion and physiological signals for the postpandemic era: a review. *Advanced Materials Technologies* 7, 12 (2022), 2200318.

[62] Martin Weigel, Tong Lu, Gilles Bailly, Antti Oulasvirta, Carmel Majidi, and Jürgen Steimle. 2015. Iskin: flexible, stretchable and visually customizable on-body touch sensors for mobile computing. In *Proceedings of the 33rd Annual ACM Conference on Human Factors in Computing Systems*. 2991–3000.

[63] Martin Weigel, Aditya Shekhar Nittala, Alex Olwal, and Jürgen Steimle. 2017. Skinmarks: Enabling interactions on body landmarks using conformal skin electronics. In *proceedings of the 2017 CHI Conference on Human Factors in Computing Systems*. 3095–3105.

[64] Li Weihao. 2021. *Modular Microfluidic Circuitry Via 3D Printing and Its Applications*. Ph. D. Dissertation. National University of Singapore (Singapore).

[65] Michael Wessely, Ticha Sethapakdi, Carlos Castillo, Jackson C Snowden, Ollie Hanton, Isabel PS Qamar, Mike Fraser, Anne Roudaut, and Stefanie Mueller. 2020. Sprayable user interfaces: Prototyping large-scale interactive surfaces with sensors and displays. In *Proceedings of the 2020 CHI Conference on Human Factors in Computing Systems*. 1–12.

[66] Michael Wessely, Theophanis Tsandilas, and Wendy E Mackay. 2016. Stretchis: Fabricating highly stretchable user interfaces. In *Proceedings of the 29th Annual Symposium on User Interface Software and Technology*. 697–704.

[67] Te-Yen Wu and Xing-Dong Yang. 2022. iWood: Makeable Vibration Sensor for Interactive Plywood. In *Proceedings of the 35th Annual ACM Symposium on User Interface Software and Technology*. 1–12.

[68] Zhiyi Wu, Tinghai Cheng, and Zhong Lin Wang. 2020. Self-powered sensors and systems based on nanogenerators. *Sensors* 20, 10 (2020), 2925.

[69] Zheer Xu, Weihao Chen, Dongyang Zhao, Jiehui Luo, Te-Yen Wu, Jun Gong, Sicheng Yin, Jialun Zhai, and Xing-Dong Yang. 2020. Bitiptext: Bimanual eyes-free text entry on a fingertip keyboard. In *Proceedings of the 2020 CHI Conference on Human Factors in Computing Systems*. 1–13.

[70] Humphrey Yang, Danli Luo, Kuanren Qian, and Lining Yao. 2021. Freeform Fabrication of Fluidic Edible Materials. In *Proceedings of the 2021 CHI Conference on Human Factors in Computing Systems*. 1–10.

[71] Huizhong Ye, Chi-Jung Lee, Te-Yen Wu, Xing-Dong Yang, Bing-Yu Chen, and Rong-Hao Liang. 2022. Body-centric NFC: Body-centric interaction with NFC devices through near-field enabled clothing. In *Designing Interactive Systems Conference*. 1626–1639.

[72] Youbin Zheng, Li Cheng, Miaomiao Yuan, Zhe Wang, Lu Zhang, Yong Qin, and Tao Jing. 2014. An electrospun nanowire-based triboelectric nanogenerator and its application in a fully self-powered UV detector. *Nanoscale* 6, 14 (2014), 7842–7846.